Effect of manufacture conditions on reverse osmosis desalination performance of polyamide thin film composite membrane and their spiral wound element

Article *in* Desalination and Water Treatment · January 2017

DOI: 10.5004/dwt.2017.20293

CITATIONS
23

READS
3,473

5 authors, including:

Abdel-Hameed Mostafa El-Aassar
Egyptian Desalination Research Center of Excellence
37 PUBLICATIONS **249** CITATIONS
SEE PROFILE

Mohamed E. A Ali
Desert Research Center
49 PUBLICATIONS **478** CITATIONS
SEE PROFILE

Yosra Kotp
Desert Research Center
29 PUBLICATIONS **393** CITATIONS
SEE PROFILE

Hosam Shawky
Desert Research Center
59 PUBLICATIONS **1,225** CITATIONS
SEE PROFILE

Desalination and Water Treatment
www.deswater.com

doi:10.5004/dwt.2017.20293

(2017) 1–7

Effect of manufacture conditions on reverse osmosis desalination performance of polyamide thin film composite membrane and their spiral wound element

Abdel-Hameed M. El-Aassar, Moustafa M. S. Abo ElFadl, Mohamed E. A. Ali, Yousra H. Kotp, Hosam A. Shawky*

Egyptian Desalination Research Center of Excellence (EDRC), Desert Research Center, Cairo, P.O.B 11753, EGYPT, Tel. +20 1002930710, Fax +20 226389069, email: Hameed_m50@yahoo.com (A.-H.M. El-Aassar), mmaboelfadl@hotmail.com (M.M.S. Abo Elfadl), m7983ali@hotmail.com (M.E.A. Ali), yoso20002000@yahoo.com (Y.H. Kotp), Shawkydrc@hotmail.com, Hashawky@edrc.gov.eg (H.A. Shawky)

Received 3 June 2016; Accepted 24 October 2016

ABSTRACT

Manual operation manufacture line was used to study the performance of flat sheet and spiral wound thin-film composite polyamide-polysulfone reverse osmosis membrane. Continuous flat sheet of porous support layer was manufactured by casting PS solution on nonwoven polyester. Fabrication of TFC flat sheet membrane was achieved through interfacial polymerization of m-phenylenediamine with trimesoyl chloride on the PS support by employing a reaction line. Finally, spiral wound element was manufactured by rolling of the resulted flat sheet membrane. The fabricated flat sheet PA-TFC membranes were characterized using; ATR-FTIR, contact angle, dynamic mechanical analyzer and scanning electron microscope. Performance of the resulted flat sheet and spiral wound membrane element was investigated in terms of water flux and salt rejection using synthesized sodium chloride solution, natural brackish & saline water samples. The effect of operation condition in the casting and coating machines on the performance of the flat sheet membrane was examined. Adoptions of the rolling technique showed significant improvement on the RO performance of the membrane element. Moreover, membrane elements were evaluated for application in water desalination process using natural brackish/saline groundwater or seawater samples.

Keywords: Membrane manufacture; Reverse osmosis; Water desalination; Thin film composite; Spiral wound element

1. Introduction

Water is the irreplaceable and valuable natural resource on the earth. Moreover, it is considered as the indispensable basic material for the existence and production of mankind. Nowadays, the water shortage affects the sustainable development of the global society, economy and ecological environment [1]. Therefore, producing of fresh water in large scale is considered one of the important issues of the development countries [2]. There are two main techniques to achieve that issue, wastewater treatment and water desalination [3]. Desalination of Seawater and brackish groundwater is attracting more interest and attention, as they are the most important methods to solve the problem of water shortage [4]. The reverse osmosis (RO) process, which relies on the semi-permeable polymeric membrane to achieve molecular separation under the driving force of hydraulic pressure, is one of the most popular technologies currently being used for water desalination [5,6]. Compared to other techniques, RO technique has many advantages such as saving energy, flexibility, ability to construct small size plants [7,8]. Moreover, these membranes can be designed in flat-sheets, hollow-fiber and in the indus-

*Corresponding author.

Presented at the EDS conference on Desalination for the Environment: Clean Water and Energy, Rome, Italy, 22–26 May 2016.

trial scale they can be designed as spiral wound [9,10]. The latter one is the most common in desalination plants due to its high capability on salt rejection and water flux [11]. Flat sheet membranes is composed of three layers: non-woven polyester, polysulfone support layer and polyamide thin film layer [12]. Polyamide Thin-film composite (PA-TFC) membrane is usually obtained by the formation of an ultra-thin PA layer onto a thicker porous substrate Polysulfone (PS) [13,14]. The chemistry and performance of both the top barrier layer and the bottom PS porous substrate of the TFC membrane can be optimized to maximize the overall membrane performance for practical use. The selective PA barrier layer is formed by interfacial polymerization between aqueous phase of an aromatic Polyamine such as m-phenylenediamine (MPD) and organic phase of one or more aromatic polyacyl chlorides like trimesoyl chloride (TMC). These commercial membranes exhibit good performance in seawater desalination [15–18]. Usually, the flat sheet thin-film composite membranes should be manufactured into a module with certain configuration for practical applications such as seawater desalination and waste water treatment. The membrane modules are subsequently developed and commercially exploited. The spiral wound module is considered as the most popular one because of its advantages of lower cost, polarization, and pressure drop across the element compared with other alternative modules such as plate-and-frame, tubular, and hollow fiber [19]. The spiral wound module has a flat sheet membrane wrapped around a perforated permeate collection tube. The feed flows on surface side of the membrane, the permeate is collected on the back side of the membrane and spirals towards the center collection tube. The feed and permeate flow are separated by sealing on back side of the membranes with glue (Fig. 1). The major components of the spiral wound membrane (SWM) element are the membrane, the feed and permeate channels spacers that keep the membrane leaves apart, the permeate core tube and the membrane housing. The feed channel spacer also enhances mass transfer near the membrane, but inevitably increases pressure loss along the membrane leaf. Membrane sheets with the spacers in between are glued together on three sides to form a leaf and rolled up around the permeate tube to create the feed and permeate channels of the SWM. Pressurized module housing holds the membrane leaves in place to prevent unwinding [20].

The main objective of this work was to manufacture of TFC membranes in flat sheets and design it as spiral wound element. To achieve this goal, three semi-automatic machines; casting, coating and rolling have been used.

2. Experimental

2.1. Materials

Polysulfone beds (Udel, P 3500 LCD MP7, M.W = 77000, M_n = 22000); N, N-Dimethyl acetamide (DMAc), Fischer; 1,3,5-Benzenetricarbonyl tri-chloride, TMC (>98%), Sigma-Aldrich; m-phenylenediamine, MPD (>99%), Across; n-Hexane, Merck were used as received without purification for preparation of TFC membranes. The reinforced non-woven fabric flat sheet rolls, feed and permeate spacers, core tubes and glue were purchased from South Korea.

2.2. Methods

2.2.2. Preparation of PS supporting membrane

Polysulfone flat sheet support layers were casted onto polyester non-woven fabric sheet (1.8 × 14″) through traditional phase inversion technique using semi-automated casting machine, Fig.1a. Briefly, the casting solution of PS solutions with different concentrations of 15–20% was pre-

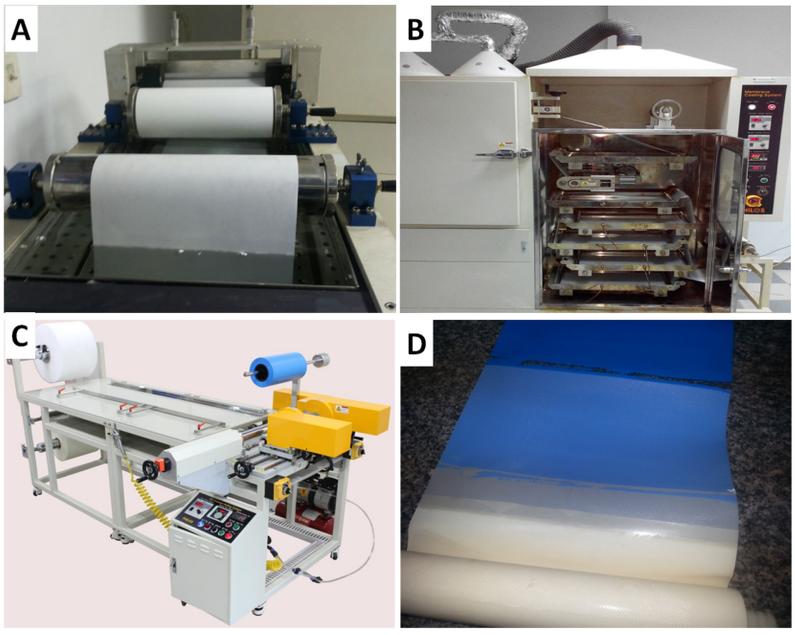

Fig. 1. Production of spiral-wound TFC membranes element; (a) PS Casting machine, (b) PA coating machine, (c) Rolling machine, and (d) Spiral wound element.

pared by dissolving the PS beads in DMAc solvent with continuous stirring at 70–80˚C. after dissolving process was completely dissolved, the casting solution was kept for specific time to degasses all air bubbles. Then the resulting polymer solution was reserved in the atmosphere until use. For fabrication of spiral wound element, the PS casting solution was putted onto the non-woven fabric with controlling the thickness (40 µm) and the temperature of the water gelation bath (25˚C). After adequate gelation time, the membranes were removed from the gelation bath and stored in distilled water to remove any excess of the solvent and non-reactant materials. These resulted membranes were ready for the next coating step.

2.2.3. Preparation of TFC membranes

The polyamide active layer was prepared onto PS porous support reinforced with polyester via in-situ interfacial polymerization technique using a pre-designed laboratory coating machine, Fig. 1b. Different solutions of MPD in water (2 wt. %) and TMC in hexane (0.15%) were used in preparation of the polyamide active layer [21,22]. For production of TFC membrane, the wet casted PS sheet was firstly passed through a bath containing aqueous MPD solution for 2 min, and then the excess solution was removed using a pressed rubber roller. Subsequently, the dried membrane was passed in TMC solution; the interaction time between MPD and TMC was fixed at 1 min. Finally the obtained TFC composite membrane was then passed through the hot air drier oven (40–50˚C).The produced membrane was washed several times with distilled water to remove all undesired reactants and kept until the next process.

2.2.4. Scale-up of the membranes

The spiral wound element was produced using laboratory rolling machine, Fig. 1c, d. During this process, the components of RO elements such as core tube; permeate spacer, flat sheet membrane, and glue were used.

2.3. Characterization of the prepared flat sheet membranes

Changes in surface chemistry of the PSF and TFC membrane surfaces were assessed by attenuated total reflectance ATR-FTIR spectroscopy (Perkin-Elemer version 10.03 spectrophotometer). The membrane surface morphology was determined using atomic force microscopy (AFM) in tapping mode (Veeco Instruments Nano-Scope, Multi-mode–V5), nd scanning electron microscope (SEM) (Quanta FEG 250 microscope). Water contact angles (VCA Video Contact Angle System, Kr Üss DSA25B (Germany) was used to determine the membrane hydrophilicity. The mechanical properties of PSF and TFC membranes were estimated using DMA TAQ800 (Film tension clamp). Thermal stability was carried out using a Shimadzu DT-60H thermal analyzer, Shimadzu, Kyoto, Japan, from ambient temperature up to 1000˚C with a heating rate of 10˚C /min.

2.4. Membrane performance

The membrane performance in terms of water flux as well as salt rejection of the prepared membranes were evaluated using laboratory RO unit (DSS-model LAB-20, Alfa lafal Corp., Denmark) with an effective area of 0.018 m^2. The flat sheet was performed using sodium chloride solution of 2000 mg/l as feed water at 10 bar as applied pressure. For spiral wound element, the membranes were performed using a designed homemade system using tab water at 4 bars.

3. Results and discussions

3.1. Membranes characterization

The ATR-FTIR was employed to analyze the chemical composition of PSF and the top surface of the TFC membrane as shown in Fig. 2. Fig. 2a shows the ATR-FTIR spectra of the PS substrate and thin film composite membranes which have polyamide top layer. FTIR spectra displaying peaks at around 835 cm^{-1} due to the in-phase out-of-plane hydrogen deformation of para-substituted phenyl groups, band at 741 cm^{-1} due to aromatic hydrogen, three neighboring, band at 1238 cm^{-1} associated with the C–O–C asymmetric stretching vibration of the aryl–O–aryl group in polysulfone. In particular peaks around 1294 cm^{-1} and 1149 cm^{-1} regions are assignable to the asymmetric SO_2 stretching vibration and symmetric stretching vibration, respectively. In addition, the peak at 3098 cm^{-1} is due to O–H aromatic stretching and the peaks at ~1583.5 cm^{-1} and 1487 cm^{-1} are associated with aromatic in-plane ring bend stretching vibration are the characteristics of PSF. Compared to the PSF substrate, two new bands at 1736 cm^{-1} and 1544 cm^{-1} appeared on the ATR-FTIR spectra for the thin film composite (TFC) membranes comprising of a polyamide surface layer as shown in Fig. 2b. This is expected because of the interfacial reaction between MPD and TMC to produce a polyamide skin layer. The small band at 1675 cm^{-1} (amide I) is present that is characteristic of C=O band of an amide group, C–N stretching, and C–N–C deformation vibration in a secondary amide group [23]. The bands from 1039–1236 cm^{-1} are characteristic of C–N bending and 1487 cm^{-1} (aromatic ring breathing), 858 cm^{-1} (aromatic hydrogen, iso-

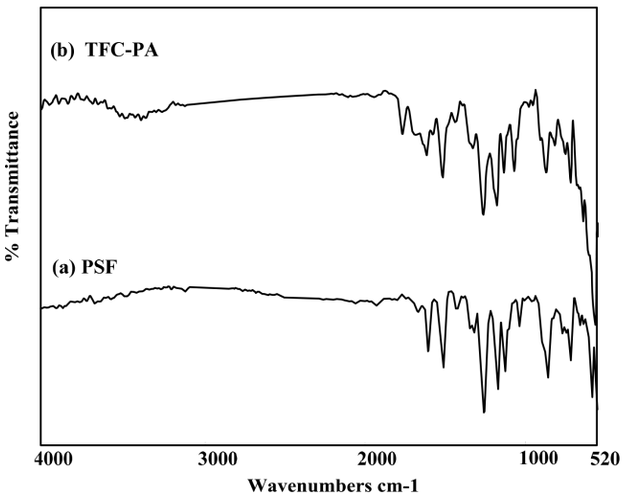

Fig. 2. ATR-FTIR spectra of PSF support layer and TFC-PA membrane.

lated) and 781 cm^{-1} (aromatic hydrogen, three neighboring). Also, the stretching peak at 3372–3474 cm^{-1} can be assigned to N–H (and O–H) and suggests several loose associative features like NH . . . N hydrogen bonds as also NH . . . O=C hydrogen bonds and peak at 3095.4 cm^{-1} assigned to O–H aromatic stretching bands [24–26].

The roughness of the outer surface of the PSF and TFC membranes was determined by AFM, Fig. 3. From the figure it was shown that the surface morphology that the surface of TFC membrane is smoother than that of pure polysulfone. Table 1 summarizes the surface roughness parameters in terms of R_a, R_q and R_{p-v} for substrate PSF, TFC membranes. The mean roughness (R_a) and mean-square surface roughness (R_q) decrease with the formation of polyamide thin layer [27]. R_{p-v} also follows a cross trend. Generally, the TFC membrane has improved hydrophilicity, smoothened surface, smaller surface pores and narrower pore size distribution compared to the PSF substrate [28,29]. These improvements affect on the formation of the selective polyamide layer and influence the RO performance of the resultant TFC membranes.

The surface morphology of TFC membrane was observed in scanning electron microscope as shown in Fig. 4. The top and transverse section of TFC membrane at different magnifications indicates clearly a top thin dense layer (selective layer) and porous thick bottom layer (support layer).The portion structure indicating crooked, worm-like strands connected with each other was attempted to correlate with the steric hindrance effect of MPD and TMC because compounds containing aromatic rings (the structure of the membrane substrate is different much before and after interfacial polymerization). Obviously the physico-chemical properties of the intermediate TFC layer may play the most important role in determining the RO performance of these membranes.

The water contact angle of the top surface of PSF substrates as well as TFC membranes were measured and observed that, in case of TFC membrane there is a rapid decrease in water contact angle from 83 (±5) of the PSF to 84° (±5) of the PSF coated TFC, Fig. 5. Furthermore, diamine may penetrate into the pores inside the PSF substrate and attach onto the pore wall via self-polymerization reaction during the TFC formation process, which can enhance their hydrophilicity [30,31]. Mechanical testing on the rectangular strip of the flat sheet PSF and TFC membranes after peeling the nonwoven polyester layer were carried out at 25°C. The mechanical properties of the synthesized membranes are presented in Fig. 6 and Table 2. The Young's modulus is calculated from the initial slopes of the linear portion of the stress–strain isotherm

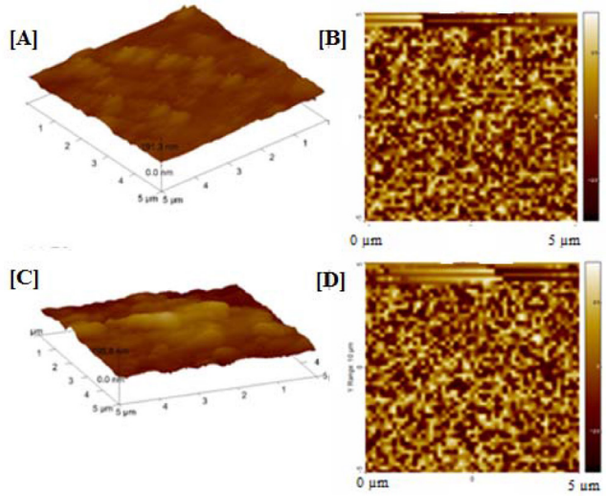

Fig. 3. 2-D (left) and 3-D (right) of AFM images of PS support membrane (A, B) and TFC membrane (C, D).

Table 1
Average measured membrane surface properties via AFM

Parameter	PSF	TFC
R_a, nm	130.5	21
R_q, nm	161	35.3
R_{p-v}, nm	104	228.3
Av. Pore diameter, nm	1186	195.8
Av. pore area, nm^2	1899901	60930.9
Tot. scan area, nm^2	2.5	2.5

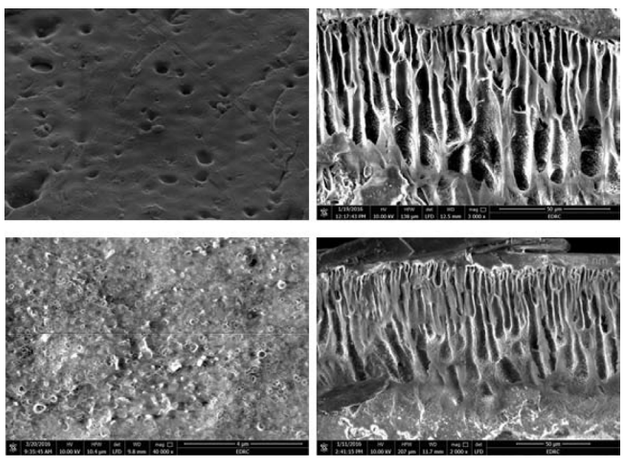

Fig. 4. SEM of surface & cross-section PSF (upper raw), surface and cross section of TFC-PA membranes (lower raw).

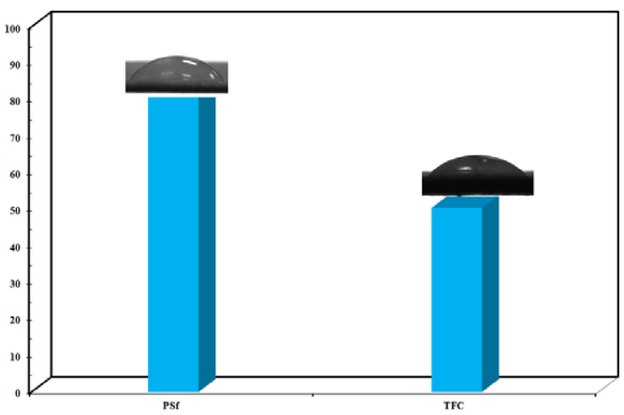

Fig. 5. Contact angle measurement of PSF and TFC membrane.

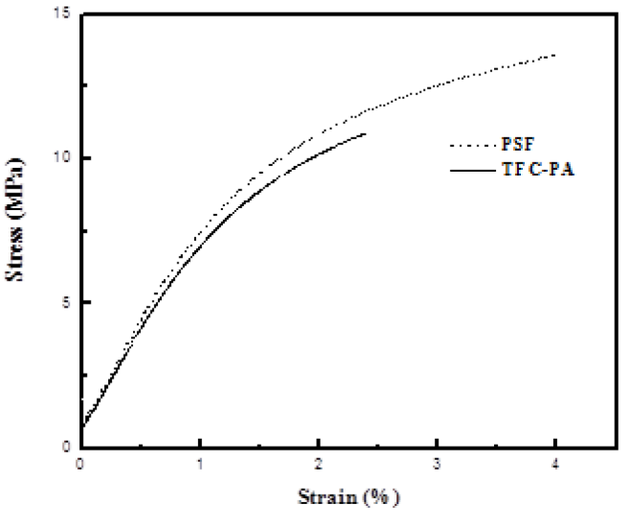

Fig. 6. Stress-Strain curve for non-woven polyester, PSF and TFC-PA membranes conditions, Ramp force 1 to 18 N, Temp 28.3, Displacement = –16353.2 um.

Table 2
Mechanical properties of PS and TFC membranes

Sample	PSF	TFC
Tensile strength, MPa	13.58	10.88
Elongation, %	4.28	2.38
Young's modulus, MPa	549.30	482.60

[32]. The results of the mechanical properties show that, PSF have a high value in Tensile strength, Elongation and Young's modulus compared to TFC membrane. This result may attribute to the less crystalline structure of polyamide layer and the mechanical properties are largely dependent on the microstructure and intermolecular forces among the chains [32].

Thermo gravimetric analysis (TGA) of PSF and TFC membranes without PET non-woven fabric were performed under nitrogen atmosphere as shown in Fig. 7. In both PSF and TFC membranes, two weight-loss stages can be observed in the TGA curve; the first stage at 451.4–561.97°C and 304.70–551.94°C for PSF and TFC respectively, was taken as the splitting of $–SO_3H$. In addition the weight loss is equal to 46.8% and 39.7% for PSF and TFC membranes, respectively, due to evaporation of additives (the boiling point of N,N dimethyl acetamide is 165°C) [33]. The second stage at above 729.9°C and 760°C is related to the splitting of the polymer main chain that accompanied by a weight loss equal to 41.92% and 58.15% for PS and PS/TFC membranes, respectively. The increasing of the weight loss compared to PSF is related to the splitting of the polymer main chain resulting in the final material carbon, which is obtained at more than 600°C. The reasons for such stability of TFC membrane is expected to originate primarily from their chemical structure, which is composed of building units generally known to be highly resistant to increased temperatures, such as amide groups and aromatic moieties (benzene rings) [34].

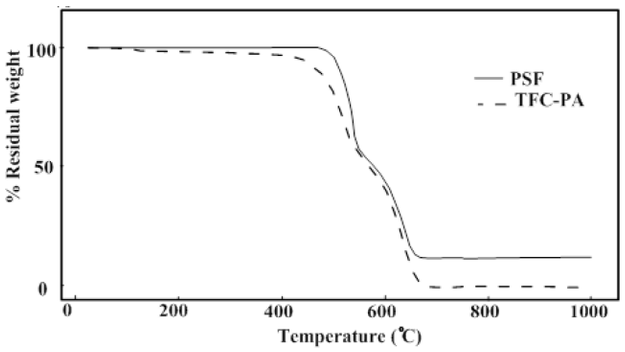

Fig. 7. TGA curves of PSF and TFC-PA with the heating rate of 10°C/min.

3.2. Membrane scaling up

There are three main components in TFC membranes, the first one is the non-woven polyester which provides the mechanical strength; the second is the porous PS support membrane with a thickness of about 40 µm that was casted onto the non-woven polyester according to traditionally phase inversion process. PS acts as substrate to the third layer that formed onto its surface by interfacial polymerization technique between the aqueous phase of MPD and the hexane organic phase of TMC. The most preferred support is prepared from PS polymer, because it is easy to process and fairly stable against thermal, mechanical, chemical and bacterial attack. The preparation conditions that affect the properties of the flat sheet TFC membranes such as PS and monomers concentration, interfacial interaction time between MPD and TMC, curing time and curing temperature were optimized before production of the spiral wound element. The concentrations of PS, monomers and additives were optimized elsewhere [35] Table 3.

For spiral wound element, there were three semi-automated laboratory machines used; casting machine for preparation of PS membrane onto non-woven polyester, coating machine for interfacial polymerization, and rolling machine for production the final element. During the casting process, the different parameters affecting the membrane performance were PS concentration of casting solution, the motor driving speed of the casting machine and the membrane thickness. Different concentrations of PS casting solutions (15, 18, 20, 25 wt.%) were casted onto

Table 3
Optimum conditions of thin film composite membrane [21]

Parameter	Conc. and conditions
PS conc., wt. %	15
MPD conc., wt. %	2
TMC conc., wt. %	0.15
Soaking time of MPD, min	2
Reaction time between MPD and TMC, min	1
Curing time, min	10
Curing temp., °C	65

non-woven polyester sheet at two pre-determined thicknesses (30, 50 µm) and four different motor driving speeds (120, 240, 400, 560 rpm). For each produced sheet, PA active layer was prepared according to the above optimum conditions and subsequently the membrane performance was evaluated in term of water flux and salt rejection, Tables 4, and 5. The results showed that the optimum conditions of producing of PS membranes using the casting machine were as follow; PS concentration of 18 wt. %, thickness of 30 µm and the motor driving speed was 240 rpm. The water flux and salt rejection of that element were 102.3 $L/m^2 \cdot h$ and 82%, respectively. According to obtained results, the high concentration of PS (25 wt. %) and the lower motor driving speed (lower than 240 rpm) were excluded due to the defects which accompanied the produced elements.

Table 4
Effect of polymer concentration and polysulfone thickness on RO Performance at different operation conditions

Code	PS Conc. (wt.%)	Thickness (µm)	J_w ($l/m^2 \cdot hr$)	Rs (%)
TFC1	15		66	82
TFC2	18		90.7	85
TFC3	20	30	99	51.5
TFC4	25		–	–
TFC5	15		275	19.5
TFC6	18		192	67.8
TFC7	20	50	18.86	34.3
TFC8	25		–	–

Table 5
Effect of motor speed on RO Performance with different thickness at different operation time

Code	Motor speed (rpm)	Thickness (µm)	J_w $L/m^2 \cdot h$	Rs (%)
TFC9	240		90.7	85
TFC10	400	30	44.5	20.7
TFC11	560		68.2	75.5
TFC12	240		192.5	67.8
TFC13	400	50	63.2	61.5
TFC14	560		132	68.5

The coating step includes formation of PA active layer onto the top surface of PS supported non-woven polyester using automated laboratory coating machine. There are two main parameters to control the produced element; the first is the ratio between un-winder tension control and winder tension control that has been fixed at (1:5). The second is the winding speed (m/min) that controls the immersing time of PS sheet in MPD as well as the reaction time between MPD and TMC; it was 0.7 m/min. after deposition of PA layer, the membranes were subjected to heat treatment to complete crosslinking of the active layer, then they were washed and kept in water bath until the rolling step. The final step was carried out using the rolling machine to obtain the spiral wound RO membrane element of dimension (1.8 × 14″). This size is used for home filter and used at applied pressure not exceeding 4 bar. The obtained performance of the membrane elements was in the range of 55–68% salt rejection with 30–35 $l/m^2 \cdot hr$ water flux. The detailed chemical parameters of the feed and product waters for three natural samples with different salinities before and after desalination process using flat sheet membranes are shown in Table 6. From the values of TDS, it is shown that all samples are suitable for drinking because all of them are below the permissible limit according to WHO (TDS = 1000 mg/l).

4. Conclusions

The scaling-up of flat sheet TFC membranes produced by interfacial polymerization between m-phenylenediamine with trimesoyl chloride onto the top surface of PS support was achieved using complete production line that consists of three machines; casting, coating and rolling machines. The effect of different parameters of fabrication conditions such as polymer concentration, support layer thickness, speed motor that influence the performance and characteristics of the resultant membranes were studied. All the prepared membranes were characterized using FT-IR, SEM, and AFM, Contact angle and Mechanical analysis, and TGA. The water flux and salt rejection of the flat sheet membrane were 102.3 $L/m^2 \cdot h$ and 82% at 10 bar, respectively, while for spiral wound element they ranged between 30–35 $l/m^2 \cdot h$ and 55–68% at 4 bar, respectively. Moreover, the membranes are suitable to be used in desalination of natural ground and sea waters samples, where the salt rejection was 90.6, 95 and 98.5 for brackish, saline and sea water samples, respectively.

Table 6
Performance of the flat sheet membranes in desalination of brackish, saline and sea water samples

Analytical parameter		Na^+	K^+	Mg^{2+}	Ca^{2+}	HCO^{-3}	SO_4^{2-}	Cl^-	TDS
Brackish water	Feed (mg/l)	1500	28	350	893	80	360	4851	8022
	Product (mg/l)	180	5.5	8	80	5	25	450	751
	% Rejection	88	80.3	97.7	91	94	93	90.7	90.6
Saline water	Feed (mg/l)	2400	34	800	1700	150	1300	7700	15140
	Product (mg/l)	240	5	6	40	4	20	450	783
	% Rejection	90	85	99	97.6	97.3	96.9	94.1	95
Sea water	Feed (mg/l)	10750	500	1850	609	126	8966	17021	39775
	Product (mg/l)	180.0	4.5	10.0	15.0	2.0	100.0	270.0	580.0
	% Rejection	98.3	99.1	99.4	97.5	99.2	98.8	98.4	98.5

Acknowledgement

It is a pleasure to acknowledge the financial support provided by the Science and Technological Development Fund (STDF) in Egypt through Grant 5240 (Egyptian Desalination Research Center of Excellence, EDRC).

References

[1]. S.M. Reddy, et al., Finding solutions to water scarcity: Incorporating ecosystem service values into business planning at The Dow Chemical Company's Freeport, TX facility. Ecosystem Services, 12 (2015) 94–107.
[2]. M.F. Hamoda, Desalination and water resource management in Kuwait. Desalination, 138(1) (2001) 385–393.
[3]. D.İ. Çifçi, S. Meriç, A review on pumice for water and wastewater treatment. Desal. Water Treat., 57(39) (2016) 18131–18143.
[4]. M.G. Salim, Selection of groundwater sites in Egypt, using geographic information systems, for desalination by solar energy in order to reduce greenhouse gases. J. Adv. Res., 3(1) (2012) 11–19.
[5]. L.F. Greenlee, et al., Reverse osmosis desalination: water sources, technology, and today's challenges. Water Res., 43(9) (2009) 2317–2348.
[6]. C. Fritzmann, et al., State-of-the-art of reverse osmosis desalination. Desalination, 216 (2007) 1–76.
[7]. D.J. Woodcock, I.M. White, The application of pelton type impulse turbines for energy recovery on sea water reverse osmosis systems. Desalination, 39 (1981) 447–458.
[8]. A. Malek, M. Hawlader, J. Ho, Design and economics of RO seawater desalination. Desalination, 105 (1996) 245–261.
[9]. A. Ahmed, I. Moch, Seawater reverse osmosis a study in use. Desalination, 82 (1991) xx-xxi.
[10]. Y. Kamiyama, et al., New thin-film composite reverse osmosis membranes and spiral wound modules. Desalination, 51 (1984) 79–92.
[11]. D.F. Sanders, et al., Energy-efficient polymeric gas separation membranes for a sustainable future: A review. Polymer, 54(18) (2013) 4729–4761.
[12]. L. Huang, J.R. McCutcheon, Impact of support layer pore size on performance of thin film composite membranes for forward osmosis. J. Membr. Sci., 483 (2015) 25–33.
[13]. S. Mitrouli, A. Karabelas, N. Isaias, Polyamide active layers of low pressure RO membranes: data on spatial performance non-uniformity and degradation by hypochlorite solutions. Desalination, 260 (2010) 91–100.
[14]. J.E. Cadotte, Interfacially synthesized reverse osmosis membrane, 1981, Google Patents.
[15]. R.W. Baker, Membranes and Modules, in Membrane Technology and Applications, 2004, John Wiley & Sons, Ltd. p. 89–160.
[16]. J. Schwinge, et al., Spiral wound modules and spacers: review and analysis. J. Membr. Sci., 242 (2004) 129–153.
[17]. Z. Yong, et al., Polyamide thin film composite membrane prepared from m-phenylenediamine and m-phenylenediamine-5-sulfonic acid. J. Membr. Sci., 270 (2006) 162–168.
[18]. A.K. Ghosh, et al., Impacts of reaction and curing conditions on polyamide composite reverse osmosis membrane properties. J. Membr. Sci., 311 (2008) 34–45.
[19]. M. Liu, et al., Preparation, structure characteristics and separation properties of thin-film composite polyamide-urethane seawater reverse osmosis membrane. J. Membr. Sci., 325 (2008) 947–956.
[20]. S. Yu, et al., Performance enhancement in interfacially synthesized thin-film composite polyamide-urethane reverse osmosis membrane for seawater desalination. J. Membr. Sci., 342 (2009) 313–320.
[21]. M.E. Ali, et al., Thin film composite membranes embedded with graphene oxide for water desalination. Desalination, 386 (2016) 67–76.
[22]. M.E.A. Ali, F.M. Hassan, X. Feng, Improving the performance of TFC membranes via chelation and surface reaction: applications in water desalination. J. Mater. Chem. A, 4(17) (2016) 6620–6629.
[23]. Y.-N. Kwon, J.O. Leckie, Hypochlorite degradation of crosslinked polyamide membranes: II. Changes in hydrogen bonding behavior and performance. J. Membr. Sci., 282 (2006) 456–464.
[24]. H. Shawky, Performance of aromatic polyamide RO membranes synthesized by interfacial polycondensation process in a water–tetrahydrofuran system. J. Membr. Sci., 339 (2009) 209–214.
[25]. L. Shi, et al., Effect of substrate structure on the performance of thin-film composite forward osmosis hollow fiber membranes. J. Membr. Sci., 382 (2011) 116–123.
[26]. L. Yang, et al., A biomimetic approach to enhancing interfacial interactions: polydopamine-coated clay as reinforcement for epoxy resin. ACS Appl. Mater. Interf., 3(8) (2011) 3026–3032.
[27]. G. Han, et al., Thin film composite forward osmosis membranes based on polydopamine modified polysulfone substrates with enhancements in both water flux and salt rejection. Chem. Eng. Sci., 80 (2012) 219–231.
[28]. P.G. Ingole, K. Singh, H.C. Bajaj, Enantioselective polymeric composite membrane for optical resolution of racemic mixtures of α-amino acids. Separ. Sci. Technol., 46(12) (2011) 1898–1907.
[29]. P.G. Ingole, K. Singh, H.C. Bajaj, Enantioselective permeation of α-amino acid isomers through polymer membrane containing chiral metal–Schiff base complexes. Desalination, 281 (2011) 413–421.
[30]. J.T. Arena, et al., Surface modification of thin film composite membrane support layers with polydopamine: enabling use of reverse osmosis membranes in pressure retarded osmosis. J. Membr. Sci., 375 (2011) 55–62.
[31]. H. Lee, et al., Mussel-inspired surface chemistry for multifunctional coatings. Science, 318(5849) (2007) 426–430.
[32]. S. Zulfiqar, M.I. Sarwar, Soluble aromatic polyamide bearing sulfone linkages: synthesis and characterization. High Perform. Polym., 21(1) (2009) 3–15.
[33]. Y.F. Liu, Q.C. Yu, Y.H. Wu, Preparation and proton conductivity of composite membranes based on sulfonated poly (phenylene oxide) and benzimidazole. Electrochim. Acta, 52(28) (2007) 8133–8137.
[34]. S. Villar-Rodil, et al., Atomic force microscopy and infrared spectroscopy studies of the thermal degradation of Nomex aramid fibers. Chem. Mater., 13(11) (2001) 4297–4304.
[35]. M.E. Abdelfattah, Chemistry and Desalination of Groundwater in the Area between Quseir and Safaga, Eastern Desert, Egypt, in Chemistry 2014, Al-Azhar: Egypt. p. 203.

Author Query

AQ1	Kindly, provide names of all authors in References 1, 5, 6, 10, 11, 16–21, 25-27, 30, 31, 34.